Journal of Power Sources 183 (2008) 464–470

Contents lists available at ScienceDirect

Journal of Power Sources

journal homepage: www.elsevier.com/locate/jpowsour

Preparation and characterization of Ni-plated polytetrafluoroethylene plate as an electrode for alkaline fuel cell

Hirotaka Kinoshita[a,b,*], Susumu Yonezawa[a], Jae-Ho Kim[a], Masayuki Kawai[c], Masayuki Takashima[a,c], Toshihide Tsukatani[b]

[a] Department of Materials Science and Engineering, Faculty of Engineering, University of Fukui, 3-9-1 Bunkyo, Fukui 910-8507, Japan
[b] Nicca Chemical Co. Ltd., 4-23-1 Bunkyo, Fukui 910-8670, Japan
[c] Cooperative Research Center, University of Fukui, 3-9-1 Bunkyo, Fukui 910-8507, Japan

ARTICLE INFO

Article history:
Received 25 February 2008
Received in revised form 21 May 2008
Accepted 22 May 2008
Available online 28 May 2008

Keywords:
Alkaline fuel cell
Electroless plating
Polytetrafluoroethylene particle
Electrode
Impedance

ABSTRACT

At about 50 wt% Ni content, Ni-plated polytetrafluoroethylene (Ni-PTFE) particles show conductivity of 300 S m^{-1} when plated on 25 μm PTFE particles. For this study, Ni-PTFE particles were formed into the Ni-PTFE plate using heat treatment at 350 °C after 300 kg cm^{-2} pressing. The Ni-PTFE plate displayed electrical conductivity and gas permeability. The plate was used as an electrode in an alkaline fuel cell (AFC). In terms of the current density, AFC using the Ni-PTFE electrode plated with Pt or Pd by immersion plating showed improved performance.

1. Introduction

Using electroless plating method with a nonionic surfactant, Ni can be plated onto the surface of a polytetrafluoroethylene (PTFE) particle. The Ni-plated PTFE (Ni-PTFE) particles are formed into the Ni-PTFE plate, which has gas permeability and electric conductivity, by heat treatment at 350 °C after pressing [1] because Ni-PTFE particles can be mutually connected via PTFE that is extruded through a Ni film on PTFE, as presented in Fig. 1. This plate is useful as an electrode for a fuel cell that uses oxygen and hydrogen. Because Ni is easily corroded in an acid solution, Ni-PTFE plate was examined for application in this study as an electrode for alkaline fuel cells (AFCs), which use an alkaline solution as an electrolyte.

Because they operate at around room temperature, as do polymer electrolyte membrane fuel cells (PEFCs) [2,3], AFCs are attractive. Material (catalyst and electrolyte) costs of AFCs are usually lower than those of PEFCs. For that reason, AFCs offer great potential for use in commercial fuel cells. Furthermore, they require no gas humidification process for AFC operation, which has heretofore been an important problem posed by the use of PEFCs. Nevertheless, exchange of the electrolyte is necessary for running an AFC because the alkaline aqueous solution absorbs CO_2, thereby degrading its performance [2]. Generally, Ni plate or carbon plate with nickel oxide catalyst is used as the AFC electrode. The apparent electrode surface area of Ni-PTFE sheet must be larger than that of Ni plate. Furthermore, Ni-PTFE sheet has flexibility, whereas other electrodes are rigid. Therefore, AFCs with high performance can be prepared using Ni-PTFE sheet as the electrode.

Fig. 2 presents an illustration of the cell for the AFC used in this study. The electrode in this cell comprises Ni-PTFE particles. The PTFE has been used to add hydrophobicity to the gas diffusion layer (GDL) and the gas diffusion medium (GDM), in which the transportation of water is facilitated [4–7]. In addition, PTFE-bonded Raney Ni hydrogen electrodes are widely used as anodes for alkaline H_2/O_2 fuel cells [8–11]. Therefore, Ni-PTFE particles are useful as a material for fuel cell electrodes.

This paper reports fuel electrode characteristics of Ni-PTFE to expound the possibility of its use as a fuel cell electrode.

2. Experimental

As the plating core material to produce the electrode material, PTFE particles with 500 μm, 350 μm, and 25 μm average diameter particle size (Polyflon PTFE M-393, M-391S and M-25; Daikin

* Corresponding author at: Nicca Chemical Co. Ltd., 4-23-1 Bunkyo, Fukui 910-8670, Japan. Tel.: +81 776 25 8590; fax: +81 776 27 7065.
E-mail address: h-kinoshita@nicca.co.jp (H. Kinoshita).

0378-7753/$ – see front matter © 2008 Elsevier B.V. All rights reserved.
doi:10.1016/j.jpowsour.2008.05.056

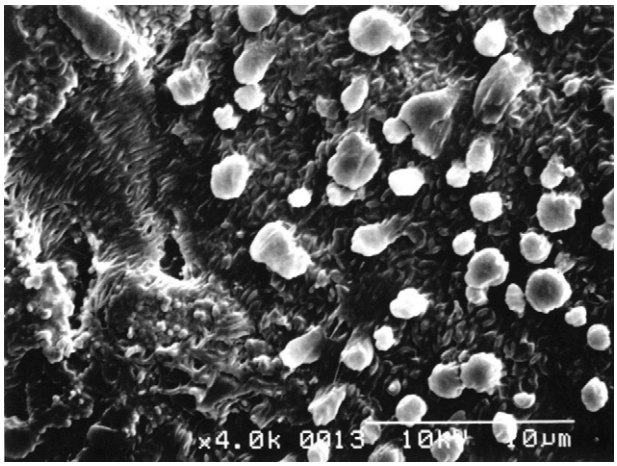

Fig. 1. SEM micrograph of surface of Ni-PTFE plate sintered after pressing.

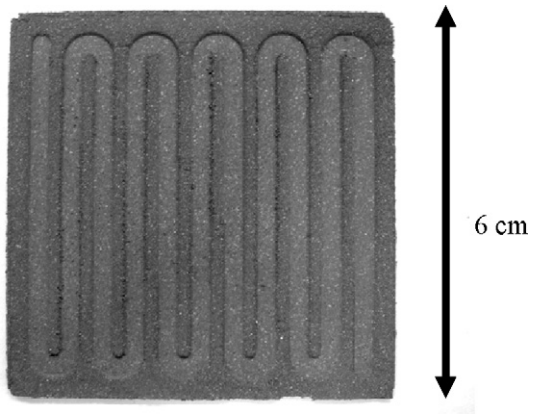

Fig. 3. Photograph of Ni-PTFE electrode.

Industries Ltd.) were selected. All particles were sieved to uniform size to prevent their mutual cohesion.

Because PTFE has low surface energy, it was hydrophilized using surfactant to disperse PTFE in a water-plating bath [1]. We used a hydrocarbon nonionic surfactant of $C_{12}H_{25}$-O-$(C_2H_4O)_2$-H (BL-2; Nikko Chemical Co. Ltd.). As the hydrophilic treatment, the PTFE particles were stirred in an aqueous solution of 2 wt% surfactant (BL-2) at 60 °C for 30 min and dried in a 70 °C air chamber after filtering and washing with ion-exchanged water.

Regarding the sensitizing process for electroless metal plating, the PTFE particles were immersed in an aqueous solution of 2 wt% tin(II) chloride dihydrate (Kanto Chemical Co. Inc.) and 1 vol.% hydrochloric acid (12 M; Nacalai Tesque Inc.) for 10 min, followed by gentle rinsing with ion-exchanged water. For the activation process, sensitized PTFE particles were immersed in an aqueous solution of 0.1 wt% palladium(II) chloride (Mitsuwa Chemical Co. Ltd.) and 0.5 vol.% hydrochloric acid (12 M) for 2 min, followed by gentle rinsing with ion-exchanged water.

The electroless plating bath was prepared using 20 g dm^{-3} nickel(II) sulfate hexahydrate (Nacalai Tesque Inc.), 30 g dm^{-3} tri-sodium citrate dihydrate (Nacalai Tesque Inc.), and sodium ammonium solution (Kanto Chemical Co. Inc.) as a pH adjuster. Then sodium phosphinate monohydrate (Nacalai Tesque Inc.) was used as the reducing agent. The activated PTFE particles, 10 g, were put into an electroless bath of 1000 ml, which was controlled at 60 °C and pH 9.0. Finally, the substrate was rinsed carefully with ion-exchanged water and dried in a 70 °C air chamber after filtering.

The conductivity of Ni-plated PTFE particles was measured using four-terminal dc method with a disk sample pressed at 3 kg cm^{-2}. The Ni-PTFE surface was observed using scanning electron microscopy (SEM, S-2400; Hitachi Ltd.). A cross-section polisher (SM-09010; JEOL) was used to observe the Ni-PTFE cross-section. The Ni amount was measured using AAS (Nacalai Tesque Inc.) from a Ni film of Ni-PTFE in nitric acid.

The electrode plate for the fuel cell was made by pressing the Ni-PTFE at 13.2 kg cm^{-2} to dimensions of 60 mm × 60 mm × 1 mm using a die with a ditch pattern to facilitate gas flow; subsequently, it was sintered at 350 °C under 10% H_2–90% N_2 and atmospheric pressure for 1 h. Fig. 3 depicts a photograph of the resultant Ni-PTFE electrode. The gas permeability of the electrode plate was measured using two methods: (1) The gas permeability measurement apparatus presented in Fig. 4 was used to measure the ratio of gas permeability. The oxygen gas flowed from the gas container to the flow meter and the amount of oxygen gas, controlled by the flow meter, was put into the permeation cell made of polypropylene carbonate. The gas permeation area of the electrode was 25 cm^2.

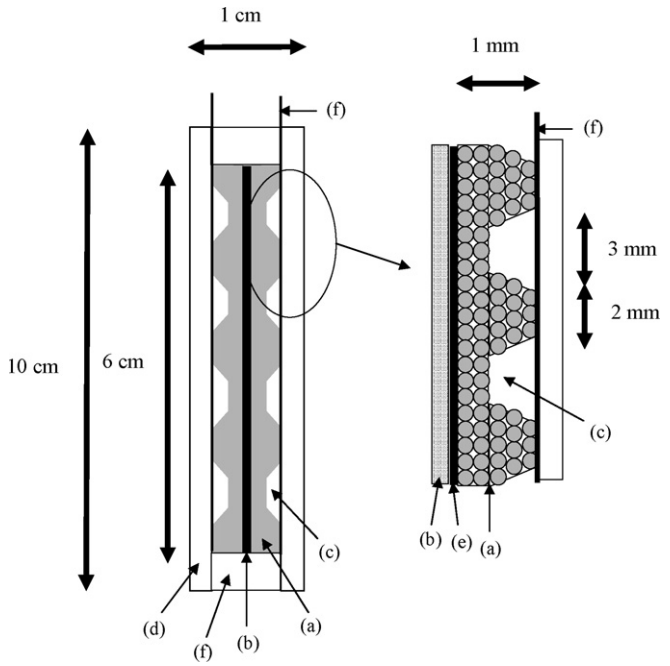

Fig. 2. Model unit cell for AFC: (a) Ni-PTFE electrode, (b) gel electrolyte, (c) gas flow channels, (d) backplate with input and output of H_2 or O_2 gas, (e) catalyst layer, (f) packing, and (g) collector.

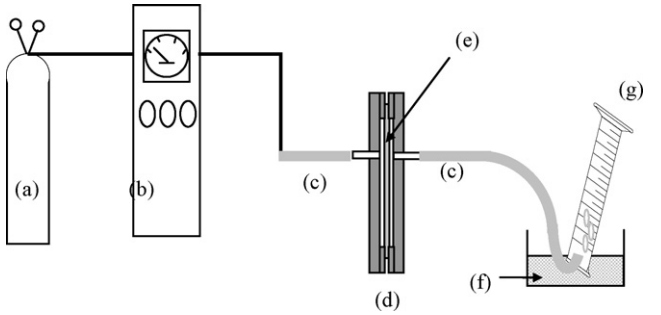

Fig. 4. Schematic diagram of the measurement apparatus of gas permeability: (a) oxygen, (b) flow meter and pressure gauge, (c) silicone tube, (d) cell, (e) electrode, (f) water container, and (g) mess cylinder.

The flow amount of gas permeated from the electrode was measured using the decreased amount of water in the mess cylinder. Subsequently, the ratio of gas permeability of the electrode was calculated from the change ratio of flow amount with an electrode and without an electrode in a cell. (2) Automated mercury porosimetry (Auto Pore IV; Micrometrics Inc., Shimadzu Corp.) was used to measure the distribution of micropores or macropores and the porosity in the electrode. In fact, EPMA-SEM analysis (S-2400; Hitachi Ltd.) was used to observe the electrode's interior structure.

Conductivity of the Ni-PTFE electrode was measured using one of two methods: (1) For the direction perpendicular to the surface of the electrode, conductivity was measured using the four-terminal dc method with a 20-mm diameter disk sample pressed at 3 kg cm^{-2}. (2) For the direction parallel to the electrode surface, the sample surface was measured directly. The conductivity was measured using four-terminal dc method with a 10 mm × 50 mm rectangular sample. In addition, Ag paste was painted to the contact point of terminal on the sample. The voltage was measured at the current of 3 mA.

The AFC unit cell was produced as presented in Fig. 2 to evaluate the Ni-PTFE for the electrode. In fact, Ni serves as a catalyst in both the anode and the cathode in AFCs, especially the cathode side. However, Pt, Pd, or Ag was generally used as a catalyst additionally: Pt or Pd was deposited on the Ni part of the Ni-PTFE plate surface by immersion plating. The Pt and Pd immersion plating baths were a 0.25 vol.% hydrochloric acid (12 M; Nacalai Tesque Inc.) solution containing 1.0 g dm^{-3} K_2PtCl_6 (Wako Pure Chemical Industries Ltd.) and 1.8 g dm^{-3} $PdCl_2$ (Wako Pure Chemical Industries Ltd.), respectively. Immersion plating was carried out for 60 min at 60 °C. The contents of Pt or Pd were measured after immersion plating using energy dispersive X-ray fluorescence spectrometry (EDX-800; Shimadzu Corp.). Platinum-loaded carbon (Pt/C; Pt-content 20 wt%; ElectroChem Inc.) of 1 mg cm^{-2} was used on the Ni-PTFE plate as a reference.

Generally, the electrolyte used was an alkaline aqueous solution. However, because a liquid electrolyte would cause liquid leakage, we used a gel electrolyte for this study. The gel electrolyte was produced by adding a gelling agent (PW-150; Nihon Junyaku Co. Ltd.) using a polymer gel electrolyte of nickel/metal hydride battery [12] or alkaline zinc cells [13,14], to 7 mol dm^{-3} potassium hydroxide (Nacalai Tesque Inc.). Fig. 2 shows that the gel electrolyte is in direct contact with the catalyst layer on the Ni-PTFE electrode.

The AFC unit cell was operated at room temperature with fuel cell performance testing equipment (PEFC single-cell testing equipment; Chino Corp.). The reaction gas flow rate was set at 100 cm^3 min^{-1} for dried H_2 gas and 200 cm^3 min^{-1} for dried O_2 gas. The cell potential properties were measured using a potentio/galvanostat (1287; Solartron Analytical).

A three-electrode AFC unit cell for impedance was constructed as presented in Fig. 5. The impedance spectra of cathode and anode were measured independently. A potentio/galvanostat (1287; Solartron Analytical) and frequency response analyzer (1260; Solartron Analytical) were used. The electrolyte was 7 M KOH, the frequency was 100 mHz to 20 kHz and the current amplitude was 1 mA cm^{-2}.

3. Results and discussion

3.1. Characterization of Ni-PTFE particles

For this study, PTFE particles of three different particle sizes (500 μm, 350 μm and 25 μm) were used to elucidate the effects of PTFE particle size on the Ni-PTFE particles' conductivity. Fig. 6 shows the conductivity of Ni-PTFE with different Ni contents. The

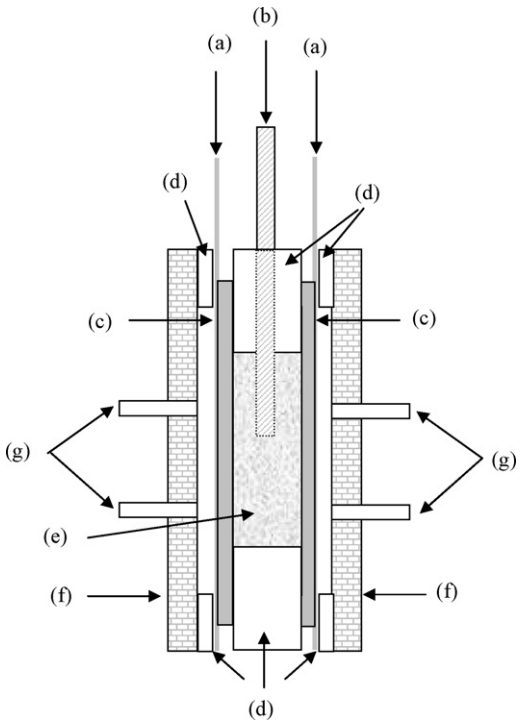

Fig. 5. Schematic illustration of a three-electrode cell for impedance measurement: (a) Ni collector, (b) reference electrode, (c) Ni-PTFE electrode, (d) seal by PTFE, (e) 7 M KOH solution, (f) backplate, and (g) input and output of H_2 or O_2 gas.

conductivity mainly increased concomitantly with increasing Ni contents for all PTFE particle sizes when the coverage of Ni was low and almost saturated. In the initial stage of the Ni plating, island-like Ni deposition occurs to conduct the low electric conductivity, as reported in a previous paper [1]. The Ni covered all surfaces of the small PTFE particle, requiring larger amounts of material than do large PTFE particles. Therefore, the Ni contents needed for complete coverage of 25 μm PTFE particle were greater than for either 350 μm or 500 μm PTFE to obtain the same conductivity. The electric conductivity of 25 μm Ni-PTFE (300 S m^{-1}) was twice that of either 350 μm or 500 μm Ni-PTFE (130 S m^{-1} or 80 S m^{-1}) when PTFE particles were covered completely with Ni. The highest conductivity was achieved using 25 μm PTFE particles. Therefore, Ni-PTFE plate was prepared using 25 μm Ni-PTFE particles in this study.

Fig. 7 depicts SEM micrographs of the surface (a) and a cross-section (b) of 25 μm Ni-PTFE particles when the Ni content was

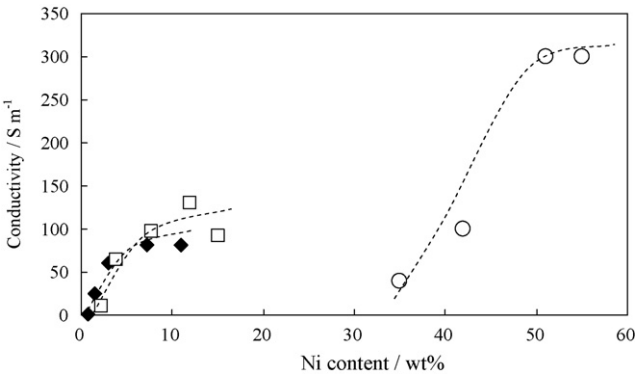

Fig. 6. Conductivity vs. Ni content of various PTFE particle sizes: (○) 25 μm, (□) 350 μm, and (♦) 500 μm.

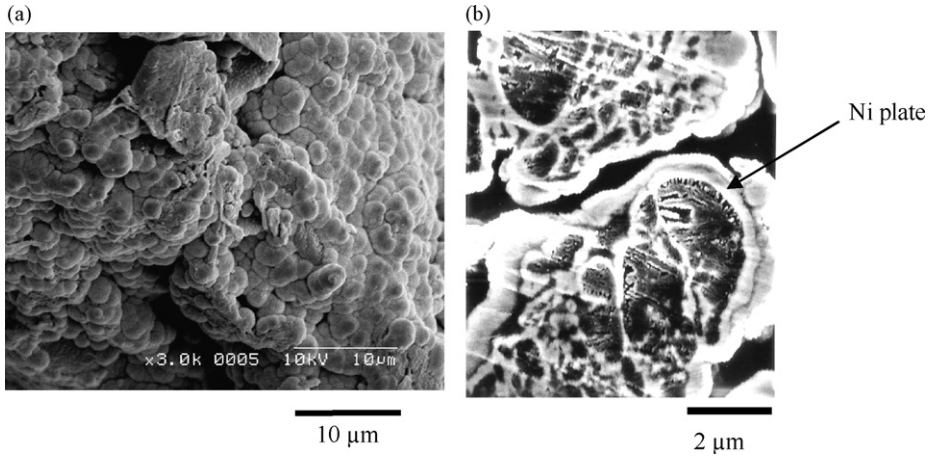

Fig. 7. SEM micrographs of Ni-PTFE particle of 51 wt% Ni content: (a) Ni-PTFE particle surface and (b) Ni-PTFE particle cross-section.

51 wt%. Fig. 7(a) shows that the Ni covered all surfaces of the PTFE particle uniformly. The boundary face of plating Ni on PTFE is clearly visible. The conductive path was apparently constructed by connecting Ni deposited on the PTFE particles; the grain boundary was closed together and had sufficient electrical contact. Using observations of the cross-section (Fig. 7(b)), the Ni film thickness was measured as ca. 1 μm. The 25 μm PTFE particle was easily aggregated. The Ni-plating film was formed on several aggregated PTFE particles. The aggregated PTFE particle diameter can be greater than 100 μm. The electric conductivity of Ni-PTFE particle can be improved through fine dispersion of the PTFE particles.

3.2. Characterization of Ni-PTFE electrode

Fig. 8 shows the pore diameter distribution of the Ni-PTFE electrode produced by 350 °C sintering after 500 kg cm^{-2} pressing, with various Ni contents, using mercury porosimetry. The porosities of each Ni-PTFE electrode have two distinctive regions in which the pore volume increases sharply: 1–10 μm, which are designated as macropores, and 0.01–0.1 μm, which are micropores [15]. The pore volume of macropores increased as Ni contents increased. The pore volume of micropores was almost independent of the Ni content. Apparently, macropores corresponded to pores along the boundary between two particles and those among several particles; micropores corresponded to grain boundaries, reflecting the roughness of the Ni film deposited on the PTFE particle [1].

The volume ratio of micropores in the Ni-PTFE electrode and its average pore size increased as Ni contents increased. Apparently, PTFE flowed easily and transformed to fill the interstitial space of Ni-PTFE particles when Ni-PTFE particles were sintered in the case of low Ni content. On the other hand, the size and the volume ratio of micropores were constant for various Ni contents. Micropores must be formed because of the roughness of the Ni surface on PTFE. The surface structure of Ni film on PTFE was unaffected by the Ni contents of Ni-PTFE. It is important to increase macropores of 1 μm [1]. However, the Ni-PTFE electrode became more fragile with increased Ni contents, although increasing the Ni contents increased the gas permeability of the Ni-PTFE electrode. An illustration of the gas permeability measurement apparatus is presented in Fig. 4; the results are presented in Table 1. Blank data (100%) were obtained by measuring the gas flow rate without the Ni-PTFE electrode. Both the 42 wt% and 55 wt% Ni-PTFE with 300 kg cm^{-2} pressing electrodes had a greater than 99% gas permeability ratio. The 42 wt% Ni-PTFE was applied as an AFC electrode in this study because the 55 wt% Ni-PTFE electrode was much more fragile than that of the 42 wt%; the 55 wt% Ni-PTFE electrode was the best in terms of gas permeability. Fig. 9 shows the pore diameter distribution for the Ni-PTFE (42 wt% Ni content) electrode, which was produced under various pressures by sintering after pressing. The pore volume and size of micropores, with pore size diameters of 0.01–0.1 μm, were almost independent of the forming pressure. The pore volume of macropores, with 1–10 μm pore diameter, increased concomitantly with the decrease in the forming pressure. The greater the pressure during the pressing process, the lower the gas permeability of the plate. It is therefore important to control the pore distribution to optimize the gas permeability of the Ni-PTFE plate. However, because the Ni-PTFE electrode was very fragile less than 300 kg cm^{-2}, 300 kg cm^{-2} was selected as the pressure to prepare the electrode for the AFC test cell used for this study.

Fig. 10 shows an SEM micrograph of the cross-section of the Ni-PTFE electrode with sintering after 300 kg cm^{-2} pressing.

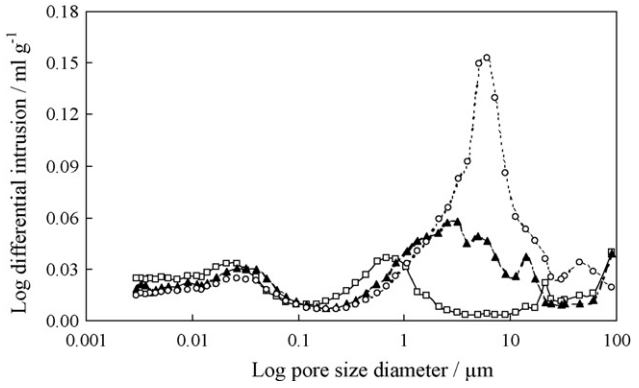

Fig. 8. Plot of the log pore diameter against log differential intrusion by mercury porosimetry for Ni-PTFE electrodes with various Ni contents: (○) 55 wt%, (▲) 42 wt%, and (□) 33 wt%.

Table 1
Gas permeability of Ni-PTFE electrode measured using the gas permeability apparatus depicted in Fig. 4

Ni-PTFE electrode	Oxygen pressure (MPa)	Gas permeability (%)
42 wt% Ni content; 300 kg cm^{-2} pressing	0.04	99
	0.08	99
42 wt% Ni content; 500 kg cm^{-2} pressing	0.04	95
	0.08	95
55 wt% Ni content; 300 kg cm^{-2} pressing	0.04	99
	0.08	99

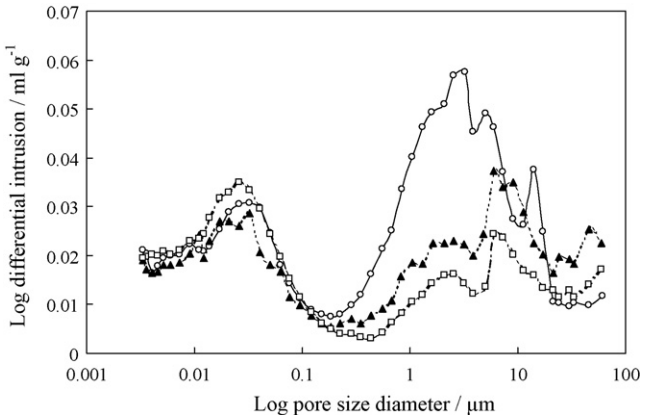

Fig. 9. Plot of the log pore diameter against log differential intrusion by mercury porosimetry for Ni-PTFE (42 wt% Ni content) electrodes with various pressure: (○) 300 kg cm^{-2}, (▲) 500 kg cm^{-2}, and (□) 1000 kg cm^{-2}.

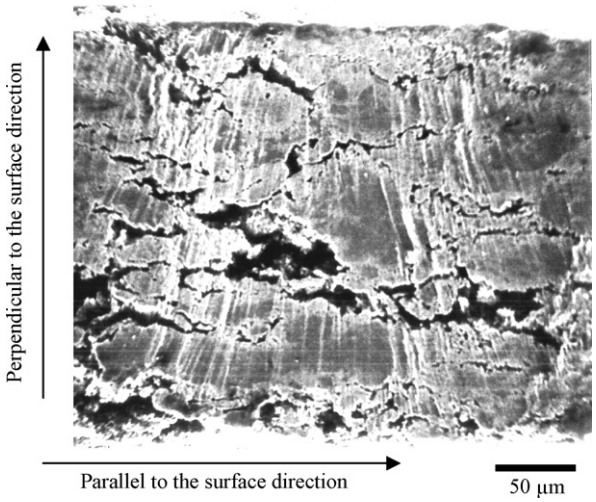

Fig. 10. SEM micrograph of cross-section of Ni-PTFE electrode sintered after 300 kg cm^{-2} pressing (42 wt% Ni contents).

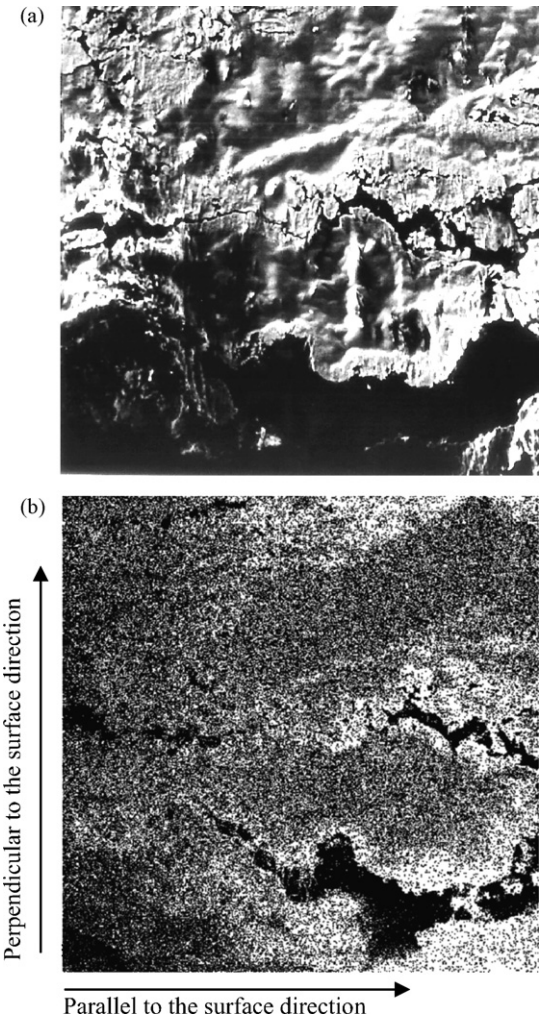

Fig. 11. (a) SEM micrograph and (b) Ni mapping image of cross-section of Ni-PTFE electrode of 42 wt% Ni content.

The Ni-PTFE particles might connect mutually via PTFE that was extruded through the Ni film on PTFE. Gaps of 10–50 μm were detected; the reaction gases might transfer through such gaps. The conductivity in the direction parallel to the electrode surface is assumed to be higher because Ni networks were created during hot pressing in this direction. Both Ni-rich and Ni-poor layers were present in the Ni-PTFE electrode and were parallel to the surface. However, the conductivity in the direction perpendicular to the electrode surface might be lower because of the presence of a Ni-poor layer along the electron transfer path. The conductivity of the Ni-PTFE electrode is presented in Table 2. The conductivity in the direction perpendicular to the surface increased with increasing Ni contents. However, the conductivity in the direction parallel to the surface had a maximum value of about 5.6×10^3 S m^{-1} at 42 wt% of Ni content. The conductivity was inferred to have decreased because of the increased number of macropores in the electrodes.

For a cross-section of Ni-PTFE electrode containing with 42 wt% Ni content, Fig. 11(a) portrays a SEM micrograph and Fig. 11(b) shows a Ni mapping image. The mapping image shows that the Ni networks in the Ni-PTFE electrode were connected along the direction parallel to the surface. Table 2 shows that the conductivity in the direction parallel to the surface is higher than that in the direction perpendicular to the surface.

Table 3 presents the current densities at 0.3 V of the AFC using Ni-PTFE electrodes after various surface treatments. The Pt-loaded carbon (Pt/C) was generally used as an electrode of the AFC and was selected as a reference. The current density of the Ni-PTFE electrode

Table 2
Conductivity of the Ni-PTFE electrode with various Ni contents

Ni contents (wt%)	Conductivity (S m^{-1})	
	Perpendicular to the surface direction	Parallel to the surface direction
33	24	0.82×10^3
42	93	5.64×10^3
55	205	1.78×10^3

Table 3
Current density of AFC using Ni-PTFE electrode at 0.3 V

	Immersion plated metal on Ni-PTFE		Current density (mA cm^{-2})
	Anode electrode	Cathode electrode	
(a)	None	None	2.0
(b)	Pt	Pt	4.8
(c)	Pt	Pd	5.2
(d)	Pd	Pt	6.0
(e)	Pd	Pd	5.6
(f)	Pt/C	Pt/C	6.4

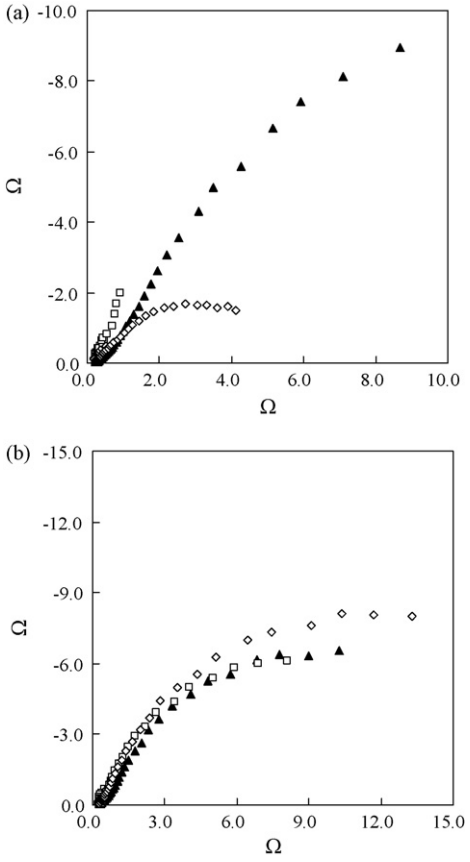

Fig. 12. Nyquist plots using various Ni-PTFE electrodes as (a) anode and (b) cathode: (▲) Pt/C painted on Ni-PTFE plate, (□) Pt immersion-plated Ni-PTFE plate, and (○) Pd immersion-plated Ni-PTFE plate.

with no surface treatment was less than half the values for other electrodes, which indicates that the catalytic performance of Ni was insufficient for AFC; still, this performance can be improved by a very slight amount of Pd or Pt deposition. By immersion plating, Pt and Pd were deposited at about 11 wt% and 7 wt%, respectively, on Ni-PTFE plate: 0.097 mg cm^{-2} and 0.062 mg cm^{-2} of Pt and Pd were deposited, respectively. These values are less than the content of Pt in Pt/C, 0.2 mg cm^{-2}. Either Pt or Pd was deposited on the Ni-PTFE while Pt/C was painted. Therefore, it seemed that the interface resistance of Pt or Pd to Ni-PTFE surface was less than that of Pt/C. In addition, the thickness of the Pt/C layer (Table 3, (f)) was estimated as about 30 μm. Because all Pt/C layer works as electrode, the net thickness of the electrode may be regarded about 30 μm. On the other hand, Pt- and Pd-deposited layer (Table 3, (d)) was estimated as less than 1 μm. It might be expected that Ni-PTFE electrode has an advantage as the material to make more compact AFC after improving its bulk conductivity and gas permeability. The impedance measurement was carried out to elucidate the electrode process for each case.

The impedance spectra were measured separately for the anode and cathode using the three-electrode AFC unit cell presented in Fig. 5. Fig. 12 presents a Nyquist plot obtained using a Pt-plated or Pd-plated Ni-PTFE electrode as an anode in panel (a) and as a cathode in panel (b). The equivalent circuit used here is presented in Fig. 13. The constant phase element (CPE) was used because the semicircle of the Nyquist plot was oval [16–27]. The fitting parameters of the impedance measurements are presented in Tables 4 and 5.

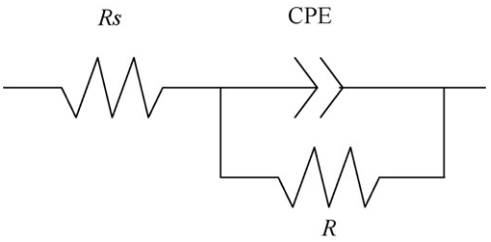

Fig. 13. Equivalent circuit used for analyzing the impedance data: Rs, resistance; *R*, charge-transfer resistance; CPE, constant phase element.

Table 4
Fitting parameter of impedance as anode

Catalyst	Load current (mA cm^{-2})	Rs (Ω)	*R* (Ω)	CPE-T (F cm^{-2})	CPE-P
Pt/C	0	0.64	34	0.099	0.76
	2	0.64	32	0.095	0.76
Pt	0	0.30	6.0	0.73	0.93
	2	0.30	11	0.70	0.90
Pd	0	0.28	5.4	0.12	0.68
	2	0.25	5.8	0.13	0.67

The CPE impedance is given by the following equation [18,21–22]:

$$Z(\mathrm{CPE}) = [T(\mathrm{j}\omega)^p]^{-1} \quad (1)$$

In this equation, $\mathrm{j} = (-1)^{0.5}$, p is an adjustment parameter, and T is the admittance constant. A CPE is commonly adopted in the model in place of a capacitor to compensate for the heterogeneity of an electrode or an interface in the system. For $p = 1$, the Z(CPE) is identical to the impedance of capacitor. For $p = 0.5$ it can be adopted to generate an infinitely long Warburg element. For the extreme case of $p = 0$, it is identical to that of a resistor. Consequently, a smaller p corresponds to a greater deviation of the element from a perfect capacitor. The porous structure of the catalyst layer was reflected on its adjustment parameter, CPE-P. For a porous electrode or rough interface, the value of p is typically 0.5–1.0 [17,18].

Actually, CPE-P is a parameter originating from surface roughness. In both the anode and the cathode, the surface roughness values, as evaluated from the CPE-P value for Pt/C-painted and Pd-plated electrodes, were higher than that of the Pt-plated electrode. Considering the surface roughness, it seemed that the apparent performance of the Pd-plated electrode was better than that of the Pt-plated one. That inference is supported by the results shown in Table 3 ((b) and (e)). The construction of the Pt/C electrode (especially the thickness of the electrode) differs greatly from that of Pd-plated or Pt-plated electrode in the case of Pt/C. Therefore, the total electrode performance of Pt/C (Table 3, (f)) cannot be discussed directly compared to those of Pd-plated and Pt-plated electrodes. However, it is inferred from their CPE-P values that the Pd-plated

Table 5
Fitting parameter of impedance as cathode

Catalyst	Load current (mA cm^{-2})	Rs (Ω)	*R* (Ω)	CPE-T (F cm^{-2})	CPE-P
Pt/C	0	0.60	56	0.079	0.79
	2	0.58	19	0.073	0.78
Pt	0	0.45	75	0.090	0.84
	2	0.43	15	0.089	0.86
Pd	0	0.34	63	0.047	0.79
	2	0.35	23	0.050	0.79

Ni/PTFE electrode has similar potential to that of the electrode for AFC.

In fact, Rs was mainly the resistance of electrolyte and Ni-PTFE. Therefore, it was almost the same value irrespective of the kind of the catalyst. However, Rs of Pt/C electrode was larger than that of the Pt-plated or Pd-plated electrode. The Pt/C electrode was thicker than the Pt-plated or Pd-plated electrode and so porous that the electrolyte, which exists in the fine pore, might have caused that result.

The charge-transfer resistance on the electrode is *R*. For the anode, *R* of the Pt/C electrode was larger than that of Pt-plated or Pd-plated electrode. It is known that not all Pt in the Pt/C electrode catalyzes the electrode process because Pt, which exists at a place where it is difficult for hydrogen gas to permeate, does not work fully [28–37]. For the cathode, *R* was almost the same value irrespective of the kind of the electrode. Therefore, the construction of the anode was more important to improve the electrode performance in this study, although the construction of the cathode was less important because of its low activation overpotential [38].

From these results, the Pd-plated Ni-PTFE plate can be a high-performance anode with the small charge-transfer resistance for AFC. The Pt/C electrode exhibited a larger load current at a certain potential than the Pt-plated or Pd-plated electrode. This larger load current capability might result from the large net surface of Pt/C electrode because of the large surface area of the carbon material. Therefore, the Pd-plated Ni-PTFE electrode might present an important advantage when the electrode must be very thin.

4. Conclusion

Using a nonionic surfactant, Ni was plated on the surface of PTFE fine particles by electroless plating. The Ni-PTFE particle conductivity increased concomitantly with increased Ni contents before Ni covered the surface; it was almost saturated after Ni covered the surface completely. The highest conductivity was achieved using 25 μm PTFE particles. Therefore, Ni-PTFE plate was prepared using 25 μm Ni-PTFE particles in this study.

Sintering at 350 °C after pressing of the Ni-PTFE particles formed the Ni-PTFE plate. The plate had electric conductivity and gas permeability. Those characteristics were influenced by the Ni contents of Ni-PTFE particles. The Ni-PTFE electrode became more fragile by increasing Ni contents, although the electric conductivity and the gas permeability of Ni-PTFE electrode increased. The gas permeability of Ni-PTFE electrode increased with decreasing pressure. Considering these factors, 42 wt% of Ni content and 300 kg cm^{-2} pressure were chosen as conditions for sample preparation in this study.

For this study, AFC was made using Pd-plated or Pt-plated Ni-PTFE electrodes. Also, as a reference, Pt/C electrodes were prepared on the Ni-PTFE plate and Ni-PTFE plate with no treatment. The catalytic performance of Ni-PTFE plate, which was insufficient to use in practical cell, can be improved by deposition of a small amount of Pd or Pt. And the thickness of the Pt-plated or Pd-plated Ni-PTFE electrode has an advantage compared to Pt/C painted Ni-PTFE electrode. It might be expected that Pt-plated or Pd-plated Ni-PTFE electrode has a useful material to make more compact AFC. From the results of CPE-P of constant phase element which appeared in the impedance measurement, surface roughness of Pt/C-painted and Pd-plated electrodes were higher than those of the Pt-plated one. The charge-transfer resistance on the Pd-plated or Pt-plated Ni-PTFE anode was smaller than that on the Pt/C anode.

Results show that the Pd-plated Ni-PTFE plate can be a high-performance anode with small charge-transfer resistance, which are beneficial characteristics for use in AFCs. The Pd-plated Ni-PTFE electrode might present an advantage when the electrode must be very thin or when a very small cell volume is required.

References

[1] H. Kinoshita, S. Yonezawa, J. Kim, M. Kawai, M. Takashima, T. Tsukatani, J. Fluor. Chem. 129 (2008) 416–423.
[2] E. Gulzow, M. Schulze, J. Power Sources 127 (2004) 243–251.
[3] M. Schulze, E. Gulzow, J. Power Sources 127 (2004) 252–263.
[4] S. Litster, G. McLean, J. Power Sources 130 (2004) 61–76.
[5] G.G. Park, Y.J. Sohn, T.H. Yang, Y.G. Yoon, W.Y. Lee, C.S. Kim, J. Power Sources 131 (2004) 182–187.
[6] T. Ioroi, T. Oku, K. Yasuda, N. Kumagai, Y. Miyazaki, J. Power Sources 124 (2003) 385–389.
[7] T. Kenjo, K. Kawatsu, Electrochim. Acta 30 (1985) 229–233.
[8] Sleem-ur-Rahman, M.A. Al-Saleh, A.S. Al-Zakri, J. Power Sources 72 (1998) 71–76.
[9] M.A. Al-Saleh, S. Gultekin, A.S. Al-Zakari, A.A.A. Khan, Int. J. Hydrogen Energy 21 (1996) 657–661.
[10] T. Kenjo, Bull. Chem. Soc. Jpn. 54 (1981) 2553.
[11] E. Gulzow, M. Schulze, G. Steinhilber, J. Power Sources 106 (2002) 126–135.
[12] C. Iwakura, S. Nohara, N. Furukawa, H. Inoue, Solid State Ionics 148 (2002) 487–492.
[13] Y. Sharma, A. Haynes, L. Binder, K. Kordesch, J. Power Sources 27 (1989) 145–153.
[14] R. Othman, W.J. Basirun, A.H. Yahaya, A.K. Arof, J. Power Sources 103 (2001) 34–41.
[15] H.K. Lee, J.H. Park, D.Y. Kim, T.H. Lee, J. Power Sources 131 (2004) 200–206.
[16] A. Bieberle, L.J. Gauckler, Solid State Ionics 135 (2000) 337–345.
[17] K.-T. Jeng, C.-C. Chien, N.-Y. Hsu, W.-M. Huang, S.-D. Chiou, S.-H. Lin, J. Power Sources 164 (2007) 33–41.
[18] N.-Y. Hsu, S.-C. Yen, K.-T. Jeng, C.-C. Chien, J. Power Sources 161 (2006) 232–239.
[19] J. Bisquert, G.G. Belmonte, P. Bueno, E. Longo, L.O.S. Bulhoes, J. Electroanal. Chem. 452 (1998) 229–234.
[20] P. Liu, H. Wu, J. Power Sources 56 (1995) 81–85.
[21] S.M.T. Takeuchi, D.S. Azambuja, I. Costa, Surf. Coat. Technol. 201 (2006) 3670–3675.
[22] G.W. Walter, Corros. Sci. 26 (1986) 681–703.
[23] C.-H. Kim, S.-I. Pyun, J.-H. Kim, Electrochim. Acta 48 (2003) 3455–3463.
[24] S.H. Liu, Phys. Rev. Lett. 55 (1985) 529–532.
[25] L. Nyikos, T. Pajkossy, Electrochim. Acta 30 (1985) 1533–1540.
[26] B. Sapoval, Solid State Ionics 23 (1987) 253–259.
[27] J.-P. Randin, E. Yeager, J. Electroanal. Chem. 36 (1972) 257–276.
[28] J. Prabhuram, T.S. Zhao, C.W. Wong, J.W. Guo, J. Power Sources 134 (2004) 1–6.
[29] Z. Zhou, W. Zhou, S. Wang, G. Wang, L. Jiang, H. Li, G. Sun, Q. Xin, Catal. Today 93 (35) (2004) 523–528.
[30] C.L. Hui, X.G. Li, I.-H. Hsing, Electrochim. Acta 51 (2005) 711–719.
[31] Y. Tang, L. Zhang, Y. Wang, Y. Zhou, Y. Gao, C. Liu, W. Xing, T. Lu, J. Power Sources 162 (2006) 124–131.
[32] S. Brimaud, C. Coutanceau, E. Garnier, J.-M. Léger, F. Gérard, S. Pronier, M. Leoni, J. Electroanal. Chem. 602 (2007) 226–236.
[33] E.N. Coker, W.A. Steen, J.T. Miller, A.J. Kropf, J.E. Miller, Micropor. Mesopor. Mater. 101 (2007) 440–444.
[34] C.K. Poh, S.H. Lim, H. Pan, J. Lin, J.Y. Lee, J. Power Sources 176 (2008) 70–75.
[35] K. Matsuoka, S. Sakamoto, K. Nakato, A. Hamada, Y. Itoh, J. Power Sources 179 (2008) 560–565.
[36] J. Xie, D.L. Wood III, K.L. More, P. Atanassov, R.L. Borup, J. Electrochem. Soc. 152 (2005) A1011–A1020.
[37] S. Kawaguchi, M. Kamada, A. Yamada, M. Ueda, Bunseki Kagaku 53 (2007) 981–986.
[38] J. Larminie, A. Dicks, Kaisetsu Nenryoudentisisutemu, Ohmsha, 2004, pp. 56–174.